

Mutation of Succinate Dehydrogenase Subunit C Results in Increased $O_2^{\bullet-}$, Oxidative Stress, and Genomic Instability

Benjamin G. Slane,¹ Nùkhet Aykin-Burns,¹ Brian J. Smith,² Amanda L. Kalen,¹ Prabhat C. Goswami,¹ Frederick E. Domann,¹ and Douglas R. Spitz¹

¹Free Radical and Radiation Biology Program, B180 Medical Laboratories, Department of Radiation Oncology, Holden Comprehensive Cancer Center and ²Department of Biostatistics, College of Public Health, The University of Iowa, Iowa City, Iowa

Abstract

Mutations in genes coding for succinate dehydrogenase (SDH) subunits are believed to contribute to cancer and aging, but the mechanism for this is unclear. Hamster fibroblasts expressing a mutation in SDH subunit C (*SDHC*; B9) showed 3-fold increases in dihydroethidine and dichlorodihydrofluorescein (CDCFH₂) oxidation indicative of increased steady-state levels of $O_2^{\bullet-}$ and H_2O_2 , increases in glutathione/glutathione disulfide (indicative of oxidative stress), as well as increases in superoxide dismutase activity, relative to parental B1 cells. B9 cells also showed characteristics associated with cancer cells, including aneuploidy, increases in glucose consumption, and sensitivity to glucose deprivation-induced cytotoxicity. Expression of wild-type (WT) human *SDHC* in B9 cells caused prooxidant production, glucose consumption, sensitivity to glucose deprivation-induced cytotoxicity, and aneuploidy to revert to the WT phenotype. These data show that *SDHC* mutations cause increased $O_2^{\bullet-}$ production, metabolic oxidative stress, and genomic instability and that mutations in genes coding for mitochondrial electron transport chain proteins can contribute to phenotypic changes associated with cancer cells. These results also allow for the speculation that DNA damage to genes coding for electron transport chain proteins could result in a “mutator phenotype” by increasing steady-state levels of $O_2^{\bullet-}$ and H_2O_2 . (Cancer Res 2006; 66(15): 7615-20)

Introduction

Metabolic oxidative stress results from an imbalance between steady-state levels of prooxidants [i.e., superoxide ($O_2^{\bullet-}$), hydrogen peroxide (H_2O_2), etc.] produced as by-products of oxidative metabolism and the cellular antioxidants that reduce these species (1). Gradual accumulation of oxidative damage to critical biomolecules (i.e., DNA) caused by metabolic oxidative stress is believed to contribute to genomic instability (2) as well as many aging-related diseases, including cancer (3–5). Mitochondrial electron transport chains (METC) are believed to be one of the major metabolic sources of $O_2^{\bullet-}$ and H_2O_2 in mammalian cells (6–9). This has led to the proposal that mutations in genes coding

for METC proteins could cause mitochondria to produce greater steady-state levels of $O_2^{\bullet-}$ and H_2O_2 that may contribute to critical aspects of the malignant phenotype, including genomic instability and increased glucose metabolism to generate reducing equivalents necessary for the detoxification of hydroperoxides (2, 5, 9–11).

Human paraganglioma syndrome is a clinical term used to describe a group of human neoplasias, including head and neck paragangliomas and adrenal or extra-adrenal pheochromocytomas that have been associated with mutations in genes coding for subunits (B, C, and D) of the succinate dehydrogenase (SDH) complex in METCs (12). However, the mechanism(s) responsible for SDH mutations causing paraganglioma syndrome tumors is not clear (12–16). Because METC proteins are capable of producing reactive oxygen species (ROS; i.e., $O_2^{\bullet-}$ and H_2O_2), it is possible that mutations in genes coding for SDH subunits could increase steady-state levels of ROS and metabolic oxidative stress that could contribute to genomic instability and tumorigenesis. To determine if mutation of the gene coding for SDH subunit C (*SDHC*) caused increases in steady-state levels of $O_2^{\bullet-}$ and H_2O_2 that could contribute to genomic instability, increased consumption of glucose, and increased sensitivity to glucose deprivation-induced cytotoxicity, previously well characterized parental Chinese hamster fibroblasts (B1 cells) and mutants (B9 cells) containing a single-base substitution that produced a premature stop codon resulting in a 33-amino acid COOH-terminal truncation of the *SDHC* protein were obtained as a generous gift from Dr. Immo E. Scheffler (University of California at San Diego, San Diego, CA; ref. 17).

Materials and Methods

Cell and culture conditions. B1 and B9 Chinese hamster lung fibroblast cells (passage 5 to 15) were maintained in high-glucose (4.5 g/L) DMEM with 10% fetal bovine serum (FBS; Hyclone, Logan, UT), nonessential amino acids, and gentamicin. Cultures were maintained in 5% CO_2 and humidified in a 37°C incubator.

Human *SDHC* plasmid construction. PCR-amplified human *SDHC* (*hSDHC*) cDNA was inserted into the Topo pCR 3.1 Uni vector. *SDHC* cDNA insertion and proper orientation into the plasmid was confirmed by sequencing the insert at the DNA sequencing core laboratory at The University of Iowa (Iowa City, IA) and compared against the known *hSDHC* cDNA sequence using BLAST. The results of the BLAST (sequence 6) search confirming insertion of *hSDHC* cDNA are as follows: gi|9257243|ref[NM_003001.2] *Homo sapiens* SHD complex, subunit C, integral membrane protein, 15-kDa (*SDHC*), nuclear gene encoding mitochondrial protein, mRNA length = 1,315; score = 700 bits (353), expect = 0.0; identities = 353/353 (100%); strand = plus/plus. The sequence of the vector insertion site and *hSDHC* cDNA insert is shown with the 5' and 3' flanking sequences beginning with the *Hind*III restriction site and ending with the *Eco*RI restriction site (underlined), the start and stop codons (bold), and the open reading frame cDNA insert (italicized):

Note: B.G. Slane and N. Aykin-Burns contributed equally to this work.

Requests for reprints: Douglas R. Spitz, Free Radical and Radiation Biology Program, B180 Medical Laboratories, Department of Radiation Oncology, Holden Comprehensive Cancer Center, The University of Iowa, Iowa City, IA 52242. Phone: 319-335-8019; Fax: 319-335-8039; E-mail: douglas-spitz@uiowa.edu.

©2006 American Association for Cancer Research.

doi:10.1158/0008-5472.CAN-06-0833

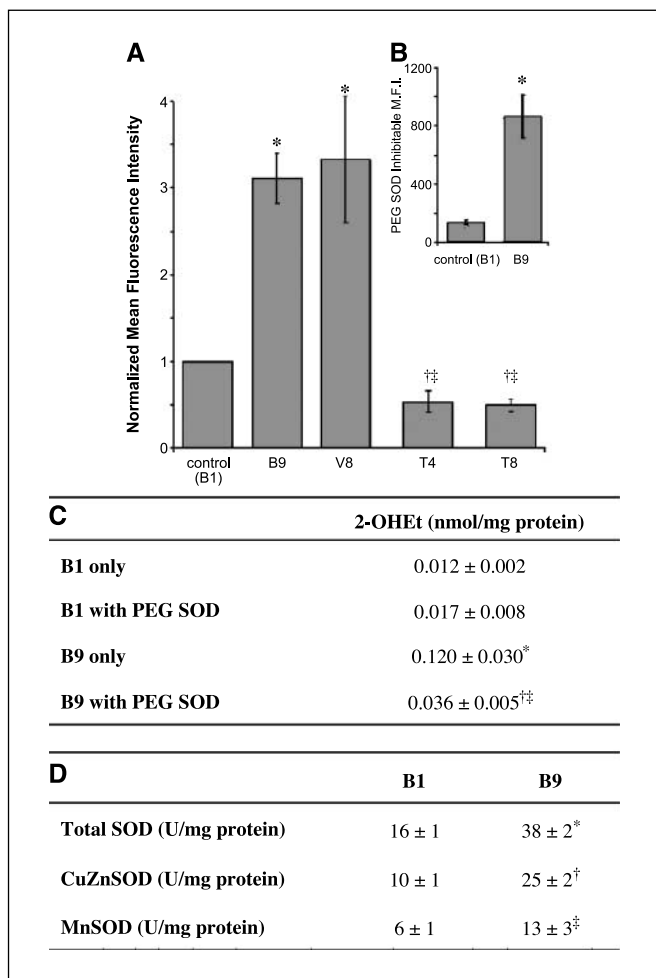


Figure 1. A, increased steady-state levels of superoxide shown by increased DHE oxidation in B9 cells as well as suppression of increased DHE oxidation shown by B9 cells overexpressing WT *hSDHC*. Cells were plated in 60-mm dishes, grown for 48 hours, and then incubated with 10 μmol/L DHE in 2 mL PBS containing 5 mmol/L pyruvate at 37°C for 40 minutes. Cells were trypsinized on ice and analyzed by flow cytometry. Each sampling measured the MFI of 10,000 cells. Values are ratio of MFI relative to B1 MFI. Columns, mean of six different experiments; bars, 1 SE. *, *P* < 0.0001, significantly different from B1, *n* = 6; †, *P* < 0.0005, significantly different from B1, *n* = 6; ‡, *P* < 0.0001, significantly different from V8, *n* = 6. B, B9 cells showed increased PEG-SOD-inhibitable DHE fluorescence relative to B1 cells. Cells were plated in 60-mm dishes, grown for 48 hours, and treated with 100 units/mL PEG-SOD for 2 hours before and during DHE labeling. Cells were trypsinized on ice and analyzed by flow cytometry. Each sampling measured the MFI of 10,000 cells. Values are ratio of MFI relative to B1 MFI. Experiment repeated twice in triplicates. Bars, 1 SD. *, *P* < 0.0001, significantly different from B1, *n* = 6. C, B9 cells showed significantly higher PEG-SOD-inhibitable 2-OHEt (superoxide-specific DHE oxidation product) relative to B1 cells. Cells were plated in 60-mm dishes, grown for 48 hours, and treated with 100 units/mL PEG-SOD for 2 hours before and during DHE labeling. Cells were trypsinized on ice and analyzed by HPLC. Values are expressed as nmol 2-OHEt/mg protein. Numbers, 1 SD. *, *P* < 0.005, significantly different from B1, *n* = 3; †, *P* < 0.01, significantly different from B9, *n* = 3; ‡, *P* < 0.05, significantly different from B1 with PEG-SOD, *n* = 3. D, B9 cells showed elevated levels of MnSOD and CuZn SOD activity compared with B1 cells. SOD activity is expressed as units per mg protein. Numbers, 1 SD from two experiments containing three separate samples. *, *P* < 0.0001, significantly different from B1, *n* = 6; †, *P* < 0.001, significantly different from B1, *n* = 6; ‡, *P* < 0.05, significantly different from B1, *n* = 6.

TTA[^]AGCTTGGAGTTACTTCCGTCAGACCCGGAACCCAAGATGGCTGC-GCTGTTGCTGAGTGCTGTTCTTTGGAAACACGGCCAAAGAAGAGATG-GAGCGGTTCTGGAATAAGAATATAGTTCAAACCGTCTCTGCTCCCA-CATTACTATCTACAGTTGGTCTCTTCCCATGGCGATGCCATCTGC-CACCGTGGCACTGGTATTGCTTTGAGTGCAGGGTCTCTTTTTGG-CATGTCGGCCCTGTTACTCCCTGGGAAGCTTGGAGTCTATTGGAACTTGT-

GAAGTCCCTGTGTCTGGGGCCAGCACTGATCCACACAGCTAAGTTG-CACTTGTCTTCCCTCTCATGTATCATACCTGGAATGGGATCCGACACTT-GATGTGGGACCTAGGAAAAGCCCTGAAGATTCCCAGCTATACCAGTCTG-GAGTGGTTGCTGTTTCTACTGTGTTGTCTCTATGGGGCTGGCAGC-CATGTGAAGAAAGGAGGCTCCAGCATAAGCCG[^]AAT.

Stable transfection of *hSDHC*. B9 cells at 60% to 70% confluence were transfected with 2.5 μg Topo pCR 3.1 Uni vector plasmid containing the *hSDHC* gene sequence or 2.5 μg empty Topo pCR 3.1 plasmid. Transfection was done using the Qiagen Superfect protocol (Valencia, CA). Clonal selection was done using the neomycin resistance gene carried on the Topo pCR 3.1 plasmid in 800 μg/mL G418. Clones were selected for isolation using a paper disc. RNA was isolated from each cell line, and reverse transcription-PCR (RT-PCR) was done at 30 cycles to confirm the cell lines were stably expressing *hSDHC* mRNA.

Measurement of intracellular superoxide levels. Superoxide production was estimated using the fluorescent dye dihydroethidium (DHE) obtained from Molecular Probes (Eugene, Oregon). Cells were washed once with PBS and labeled on culture plates at 37°C for 40 minutes in PBS (containing 5 mmol/L pyruvate) with DHE (10 μmol/L; in 1% DMSO). Culture plates were placed on ice to stop the labeling, trypsinized, and resuspended in ice-cold PBS. Samples were analyzed using a FACScan flowcytometer (Becton Dickinson Immunocytometry Systems, Inc., Mountain View, CA; excitation 488 nm, emission 585 nm band-pass filter). The mean fluorescence intensity (MFI) of 10,000 cells was analyzed in each sample and corrected for autofluorescence from unlabeled cells (18). The MFI data were normalized to B1 levels.

High-performance liquid chromatography analysis of 2-hydroxyethidium and ethidium. Dihydroethidium and the superoxide-derived oxidation product [2-hydroxyethidium (2-OHEt)] were separated on a C18 reverse-phase column (Partisil ODS-3 250 × 4.5 mm, Alltech Associates, Deerfield, IL) with a gradient system. Mobile phase was initially 10% CH₃CN in 0.1% trifluoroacetic acid, and the 2-OHEt was separated by a linear increase in CH₃CN concentration from 10% to 70% in 46 minutes at a flow rate of 0.5 mL/min. DHE/O₂⁻-specific product was detected by a fluorescence detector with excitation and emission at 510 and 595 nm, respectively (19).

Measurement of intracellular prooxidant levels (presumably hydroperoxides). Steady-state levels of prooxidants were determined using the oxidation-sensitive (CDFH₂, 10 μg/mL) and oxidation-insensitive (CDCE, 10 μg/mL) fluorescent dyes (dissolved in 1% DMSO) obtained from Molecular Probes. The cells were washed once with PBS and labeled with the fluorescent dyes for 15 minutes at 37°C in PBS. At the end of the incubation time, the plates were placed on ice to stop labeling. Cells then were harvested on ice, resuspended in PBS, and analyzed using a FACScan flow cytometer (Becton Dickinson Immunocytometry Systems; excitation 488 nm, emission 530 nm band-pass filter). The MFI of 10,000 cells was analyzed in each sample and corrected for autofluorescence from unlabeled cells (9). Expressed data were normalized to B1 levels of MFI.

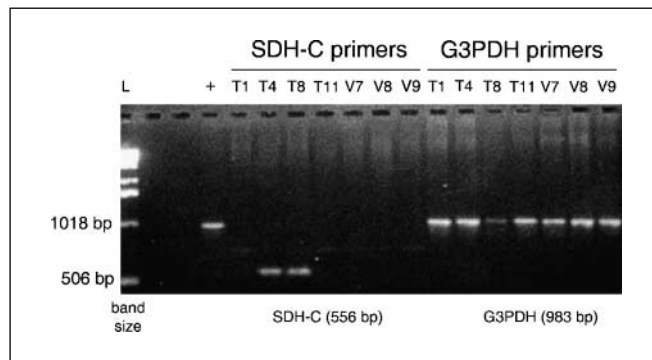


Figure 2. RT-PCR analysis confirms the expression of *hSDHC* mRNA in T4 and T8 clones. RNA was isolated from each cell line, and RT-PCR analysis was done to confirm if the cell lines were stably expressing *hSDHC* mRNA (556 bp). V7, V8, and V9 clones were used as vector controls. Glyceraldehyde-3-phosphate dehydrogenase was used as a loading control.

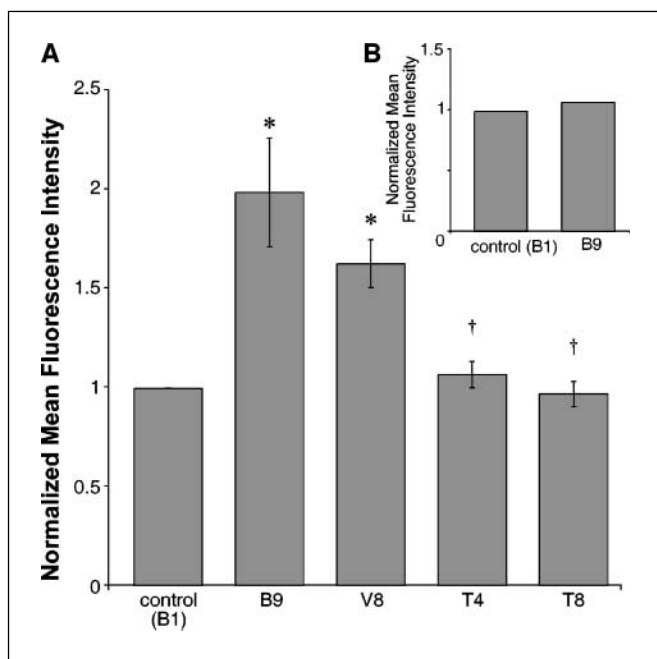


Figure 3. A, B9 cells showed significantly increased oxidation of CDCFH₂ relative to B1 cells. Cells were plated in 60-mm dishes, grown for 48 hours, and then incubated with 10 μ g/mL CDCFH₂ in 2 mL PBS at 37°C for 15 minutes. Cells were trypsinized on ice and analyzed by flow cytometry. Each sampling measured the MFI of 10,000 cells. Values are ratio of MFI relative to B1 MFI. Columns, mean of five different experiments; bars, 1 SE. *, $P < 0.05$, significantly different from B1, $n = 5$; †, $P < 0.05$, significantly different from V8, $n = 5$. B, the oxidation-insensitive probe showed no difference in fluorescence between B9 and B1 cells. Cells were plated in 60-mm dishes, grown for 48 hours, and then incubated with 10 μ g/mL CDCF in 2 mL PBS at 37°C for 15 minutes. Cells were trypsinized on ice and analyzed by flow cytometry. Each sampling measured the MFI of 10,000 cells and is expressed as the ratio of MFI relative to B1 MFI.

Superoxide dismutase activity. Total superoxide dismutase (SOD) activity was determined by the indirect competitive inhibition assay originally developed by Spitz and Oberley (20). Superoxide is generated from xanthine by xanthine oxidase and detected by recording the reduction of nitroblue tetrazolium (NBT). SOD scavenges superoxide and competitively inhibits the reduction of NBT. One unit of SOD activity is defined as the amount of protein required to inhibit 50% of the maximal NBT reduction. To obtain the amount of MnSOD activity, sodium cyanide (5 mmol/L) is added to inhibit the CuZnSOD enzyme activity.

Thiol analysis. Cells were grown to 70% to 80% confluency on 100-mm dishes and scraped in 5% sulfosalicylic acid to prevent oxidation during sample preparation. Glutathione (GSH) content was determined by the reduced GSH/GSH disulfide (GSSG) recycling method. A yellow color change is detected at 412 nm, as 5,5'-dithiobis-(2-nitrobenzoate) is converted to 2-nitro-5-thiobenzoate by the conversion of 2 GSH to GSSG. The total GSH content is proportional to the rate at which the yellow color accumulates. To determine the amount of GSSG, 2-VP (20 μ L; 1:1 mixture of 2-VP and 100% ethanol) was added to 100 μ L sample and incubated for 2 hours and assayed as described (9, 21).

Measurement of glucose consumption. Glucose consumption per cell was measured by plating 300,000 B1 and B9 cells on a 60-mm cloning dish 21% O_2 at 37°C. The cells were allowed 24 hours to recover from trypsin. Cells were given fresh medium at time zero. Cells were counted and, medium samples were obtained at 48 hours and analyzed using a YSI glucometer. Glucose consumption was determined by subtracting glucose content at 48-hour point from the time zero sample and divided by the number of cells (9).

Measurement of glucose deprivation-induced cytotoxicity. Cytotoxicity due to glucose deprivation was measured by plating 300,000 B1 and B9 cells on a 60-mm cloning dish 21% O_2 at 37°C. The cells were allowed 24 hours to recover from trypsin. At time zero, cells were given fresh glucose-

free medium containing 10% dialyzed FBS, nonessential amino acids, and gentamicin. Clonogenic survival was determined at 48 hours and normalized to time zero plating efficiency (9).

Nuclear chromosome analysis. Chromosomes were prepared according to a previously described method (22). Approximately 500,000 cells were plated in T-75 flasks. At the time of the experiment, cells were ~50% to 60% confluent and actively dividing. The cells were treated with colcemid at 0.06 μ g/mL for 3 hours. After colcemid treatment, the cells were collected by mitotic shake off and centrifuged for 5 minutes at 1,200 rpm. The pellet was resuspended in 0.075 mol/L KCl and incubated for 25 minutes at 37°C. The suspension was centrifuged, and the pellet resuspended in Carnoy's fixing solution (3:1 ethanol/glacial acetic acid) for 5 to 10 minutes. The cells were again centrifuged and resuspended in an amount of Carnoy's that gave the appropriate number of cells per slide. Suspension (100 μ L) was added to slides that had been dipped in ice water, and the slides were allowed to dry overnight. After drying, the slides were dipped into 2% aceto-orcein solution for 30 minutes at room temperature and then washed successively in 70% ethanol, 95% ethanol, and 100% ethanol. Slides were allowed to dry completely and mounted using Permount and coverslips. Slides were allowed to dry thoroughly and then counted using an oil immersion microscope.

Propidium iodide staining for DNA content measurement. Asynchronously growing exponential cultures of B1 and B9 cells were trypsinized and fixed in 70% ethanol. Ethanol-fixed cells were washed with PBS and treated with RNase A for 30 minutes followed by staining with propidium iodide (35 μ g/mL). DNA content of propidium iodide-stained cells was analyzed by flow cytometry, and the percentage of cells in each phase of the cell cycle was calculated using CellQuest Pro and WinMDI software following our previously published protocols (23).

Statistical analysis. Two-way ANOVA analysis was used to study the effects of experiment and group on outcome measurements (one-way ANOVA used for chromosomal analysis). Statistically significant global test of equality across groups was followed up with pair-wise comparisons to identify specific group differences. Tests were carried out at the 5% level of significance. Tukey's multiple comparison test was used for the pair-wise comparisons.

Results

DHE is a nonfluorescent compound used to detect $O_2^{\cdot-}$ by virtue of the fact that it is oxidized by intracellular $O_2^{\cdot-}$ to form an easily detected fluorescent product, 2-OHET (19). Figure 1A shows, using flow cytometry analysis (18), that B9 cells exhibited a 3-fold increase in oxidation of DHE to its fluorescent products when compared with B1 cells, suggesting significantly increased steady-state levels of $O_2^{\cdot-}$. To confirm if this increase in DHE oxidation (Fig. 1A) was specific for $O_2^{\cdot-}$, the flow cytometric analysis was repeated after treating the B1 and B9 cells with 100 units/mL polyethylene glycol-conjugated CuZnSOD (PEG-SOD) for 2 hours before and during DHE labeling. Results in Fig. 1B show the PEG-SOD-inhibitable DHE oxidation was increased 8-fold in B9 cells, relative to B1 cells. To further confirm increased $O_2^{\cdot-}$, 2-OHET, the specific oxidation product of $O_2^{\cdot-}$ with DHE, was analyzed by high-performance liquid chromatography (HPLC; ref. 19), and again, the difference between B1 and B9 cells was found to be ~10-fold as well as inhibitable with PEG-SOD (Fig. 1C). These results show conclusively that B9 cells expressing the mutant form of *SDHC* show significantly increased steady-state levels of $O_2^{\cdot-}$, relative to parental cells expressing the wild-type (WT) *SDHC* (B1).

To determine if increases in steady-state levels of $O_2^{\cdot-}$ in B9 cells were a direct result of expressing the mutant *SDHC* gene, B9 cells were stably transfected with a PCR-amplified WT *hSDHC* cDNA as described in Materials and Methods. The RT-PCR analysis in Fig. 2 confirmed the expression of the *hSDHC* mRNA transcript in clones T4 and T8 as well as the lack of *hSDHC* expression in vector control clones (V7, V8, and V9). When steady-state levels of $O_2^{\cdot-}$ were measured, T4 and T8 cells showed DHE oxidation similar to B1 cells

Table 1. Analysis of glutathione, glucose consumption, and glucose deprivation-induced cytotoxicity in wildtype and mutant *SDHC* expressing cells

	B9	V8	B1	T4	T8
Total GSH (fmol/cell)	418 ± 40*	293 ± 60*	85.0 ± 7	102 ± 10 [†]	107 ± 8 [†]
GSSG (fmol/cell)	13 ± 8 [‡]	6.3 ± 2	4.0 ± 1	2.4 ± 1 [§]	2.5 ± 1 [§]
Glucose consumption (nmoles glucose/cell/48 h)	16 ± 1*	18 ± 2*	3 ± 1	5 ± 1 [†]	6 ± 1 [†]
Glucose deprivation cytotoxicity (% survival at 48 h)	23 ± 1*	7 ± 1*	47 ± 3	56 ± 4 [†]	53 ± 4 [†]

NOTE: B9 and V8 cells display elevated levels of GSH and GSSG compared with B1, T4, and T8 cells. Total GSH (GSH + GSSG) as well as GSSG are expressed as femtomoles per cell in GSH equivalents using a spectrophotometric recycling assay. Errors represent ±1 SD from three experiments containing three separately collected and analyzed samples. $n = 9$.

B9 and V8 cells display increased rates of glucose consumption compared with B1, T4, and T8 cells. Glucose consumption was quantified by measuring the disappearance of glucose from the medium. Medium samples were obtained at 48 hours and analyzed by an YSI glucometer. Errors represent ±1 SE of the mean from two different experiments. $n = 6$.

B9 and V8 cells display greater sensitivity to glucose deprivation-induced cytotoxicity compared with B1, T4, and T8 cells. Cells were plated in 60-mm dishes and grown in normal complete medium for 24 hours and then changed to glucose-free medium at time zero and assayed for clonogenic survival at 48 hours. Errors represent ±1 SE of the mean from three different experiments. $n = 9$.

*Significantly different from B1, $P < 0.0001$.

[†]Significantly different from V8, $P < 0.0001$.

[‡]Significantly different from B1, $P < 0.001$.

[§]Significantly different from V8, $P < 0.0005$.

(Fig. 1A). In contrast, V8 cells displayed DHE oxidation nearly identical to B9 cells and significantly elevated relative to B1 cells. These results show that increased steady-state levels of O_2^- in B9 cells expressing the mutant *SDHC* can be reverted to levels similar to the parental B1 cells by overexpressing WT *hSDHC*. This strongly supports the conclusion that expression of the mutant form of *SDHC* is directly responsible for the increased O_2^- in B9 cells.

Mammalian cells contain a cytosolic CuZnSOD as well as a mitochondrial MnSOD that are believed to play critical roles in the detoxification of O_2^- produced as a by-product of oxidative metabolism (4, 24–29). To determine if decreases in SOD activity could contribute to the increases in steady-state levels of O_2^- in B9 cells, SOD activity analysis was done (20). B9 cells showed 2-fold increases in MnSOD and CuZnSOD activity, relative to B1 cells (Fig. 1D), as well as a similar increase in immunoreactive protein corresponding to MnSOD (data not shown). These results show that the observed increases in O_2^- were not caused by decreases in SOD activity and suggest that B9 cells have increased the expression of O_2^- -scavenging enzymes as an adaptive response to increased O_2^- caused by the mutation in *SDHC*.

To determine if steady-state levels of hydroperoxides and other prooxidants were increased in B9 cells (relative to B1) causing metabolic oxidative stress, cells were labeled with a more general oxidation-sensitive probe CDCFH₂ (9). Figure 3A shows B9 cells labeled with CDCFH₂, which show a 2-fold increase in steady-state levels of intracellular prooxidants (presumably hydroperoxides) relative to B1 cells. Again, the change in CDCFH₂ oxidation seen in B9 cells was reverted to B1 levels in clones T4 and T8 by expression of the WT *hSDHC*, relative to the V8 vector control (Fig. 3A). In addition, this experiment was repeated using CDCE, the oxidation-insensitive analogue of CDCFH₂, to control for possible changes in probe uptake, ester cleavage, or efflux, and the data in Fig. 3B show no difference in labeling between the B1 and B9 cells. These results provide strong evidence that changes seen in Fig. 3A are indicative of increased steady-state levels of probe oxidation in B9 cells, relative to B1. To determine if the increases in steady-state levels of prooxidants (presumably O_2^- and H_2O_2) in B9 cells resulted in metabolic oxidative stress, levels of total GSH and GSSG were

analyzed as described previously (9, 21). The results in Table 1 show B9 cells had significantly increased levels of total GSH and GSSG, relative to the B1 cells. Again, the changes in total GSH and GSSG seen in B9 cells reverted to B1 levels in clones T4 and T8 expressing the WT *hSDHC*, relative to the V8 vector control. These results provide strong evidence that the B9 cells expressing the mutant *SDHC* are experiencing metabolic oxidative stress. As with the SOD activity results shown in Fig. 1D, these results also suggest that the B9 cells are adapting to mutant *SDHC* expression by synthesizing more GSH but are not completely able to maintain the newly synthesized GSH in the reduced state. This supports the hypothesis that these cells are living in a condition of chronic

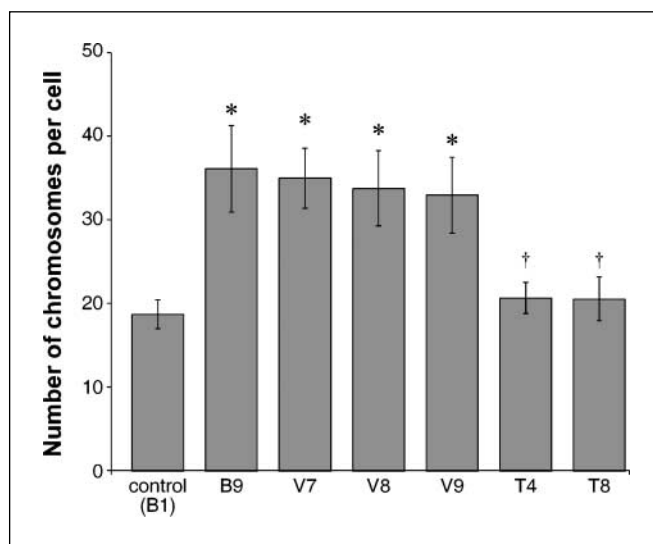


Figure 4. B9 cells showed increases in aneuploidy that were suppressed by expression of WT *hSDHC*. Whole-mount chromosomes were counted in a blinded fashion. Individual spreads were deemed countable if all chromosomes were clearly defined and clearly visible within the ghost of a single cytoplasm. Columns, mean chromosome number per cell of 100 separate counts; bars, 1 SD. *, $P < 0.0001$, significantly different from B1; †, $P < 0.0001$, significantly different from V7, V8, or V9.

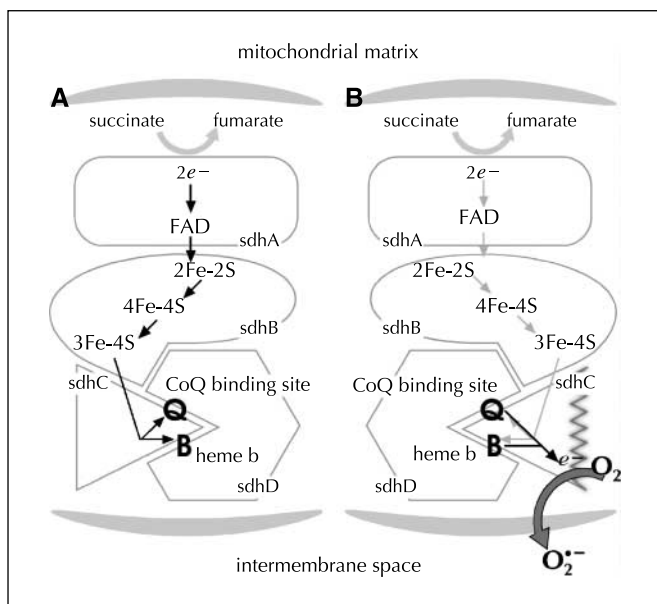


Figure 5. The proposed model of WT and mutant SDHC containing complex II with the proposed site of superoxide production. Proposed normal complex II existing in B1 cells (A) and the proposed SDHC mutant complex II present in B9 cells (B). Arrows, flow of electrons as they are passed through the flavin to the Fe-S groups and then to the CoQ-binding site or the heme b site.

metabolic oxidative stress that directly results from expressing the mutant SDHC.

Examination of cell biology variables in B9 cells expressing mutant *SDHC* revealed striking phenotypic differences when compared with the parental B1 cells. B9 cells showed a 29-hour doubling time, and B1 cells showed a 15-hour doubling time, indicating that cell growth was significantly slower in cells expressing the *SDHC* mutation. To determine if the difference in cell doubling time between B1 and B9 cells could be due to differences in cell cycle phase distribution, flow cytometry measurements of cells in G_1 , S, and G_2 -M were done (23). Asynchronously growing exponential cultures of B1 cells showed $36 \pm 0.4\%$ G_1 (mean \pm 1 SD), $28 \pm 0.2\%$ S, and $36 \pm 0.5\%$ G_2 -M. In contrast, B9 cells showed $46 \pm 1\%$ G_1 , $30 \pm 1\%$ S, and $24 \pm 0.2\%$ G_2 -M. A statistically significant increase ($P < 0.005$) in the percentage of G_1 phase was noted in B9 cells, relative to B1 cells, suggesting that B9 cells are progressing more slowly through G_1 . Interestingly, B9 cells overexpressing the WT *hSDHC* (T4 and T8 clones) displayed doubling times of 17 and 15 hours (similar to B1), whereas the V8 vector control showed a doubling time of 25 hours (similar to B9). B9 cells also showed a 5-fold increase in glucose consumption as well as significant sensitization to glucose deprivation-induced clonogenic cell killing when compared with B1 cells (Table 1). The elevated rates of glucose consumption as well as the increased sensitivity to glucose deprivation-induced cytotoxicity in B9 cells again reverted to levels similar to B1 cells in clones overexpressing the WT *hSDHC* (T4 and T8) but not in the V8 vector control clone (Table 1). Most strikingly, chromosome analysis of at least 100 metaphases (22) indicated that the B1 cells were quasidiploid with a mean chromosome number of 18 ± 2 , and the B9 cells were highly aneuploid with a mean chromosome number of 37 ± 5 (Fig. 4). The increases in aneuploidy showed by B9 cells again reverted to levels similar to B1 cells in clones overexpressing the WT *hSDHC* (T4 and T8) but not in the V8 vector control (Fig. 4). To ensure that these results were not an artifact of clonal selection, two more vector controls (V8 and V9)

were analyzed and also found to be highly aneuploid, relative to B1, T4, and T8 (Fig. 4). These results show that expression of the *SDHC* mutation caused longer cell cycle times, increased glucose consumption, increased sensitivity to glucose deprivation-induced clonogenic cell death, and increases in genomic instability (as assayed by aneuploidy) that were reversed by expression of WT *hSDHC*. This cell biology data taken together with the fact that overexpression of *hSDHC* in B9 cells decreased disruptions in GSH metabolism as well as decreased steady-state levels of $O_2^{\cdot-}$ and H_2O_2 support the hypothesis that metabolic oxidative stress was causally linked to phenotypic changes associated with the expression of the *SDHC* mutation.

Discussion

It has been proposed that metabolic production of ROS (i.e., $O_2^{\cdot-}$ and H_2O_2) could be related to the DNA-damaging processes causing aging and carcinogenesis (3, 10, 11, 30). However, the possible sources of ROS have been less well understood (3, 10, 11, 30). To account for the fact that the incidence of degenerative diseases associated with aging (including cancer) increases as an exponential function of age, it has been proposed that the gradual accumulation of ROS-induced genetic damage reaches a critical level where alterations in genes governing the accumulation of further damage causes the acceleration of the process (3, 11). This has led to the development of the concept of a "mutator phenotype" to explain the higher than predicted incidence of cancer in human populations (31). Initially, it was thought that the "mutator phenotype" leading to genomic instability could involve damage to the genes coding for proteins governing DNA repair, and evidence supporting this hypothesis is accumulating (31). Equally likely is the possibility that damage to genes coding for proteins governing the metabolic production of ROS (particularly METC proteins) could accelerate the DNA-damaging processes leading to a "mutator phenotype."

In the current study, B9 cells expressing a single-base mutation that truncates 33 amino acids from the COOH-terminal integral membrane portion of the SDHC were found to show increased steady-state levels of ROS (i.e., $O_2^{\cdot-}$ and H_2O_2). In addition, B9 cells showed increased levels of SOD activity, increased levels of total GSH and GSSG, increased glucose consumption, increased sensitivity to glucose deprivation-induced toxicity, slower growth rates, and dramatic increases in aneuploidy. These B9 phenotypic characteristics were all reversed by expression of the WT *hSDHC*. These results are consistent with the hypothesis that mutations in genes coding for electron transport chain proteins (i.e., SDHC) can lead to increased steady-state levels of intracellular ROS causing metabolic oxidative stress and genomic instability.

SDHC and SDHD are integral membrane proteins thought to anchor complex II of the electron transport chain into the inner mitochondrial membrane and facilitate transfer of electrons to coenzyme Q (CoQ; ref. 32). Consequently, the mutant SDHC protein expressed by B9 cells would be expected to potentially alter the CoQ-binding site and heme b site formed at the interface of subunits C and D (Fig. 5). Disruption of this part of the complex could result in increased accessibility of electrons (flowing toward CoQ) to molecular O_2 dissolved in the membrane, thereby increasing the probability for one-electron reduction of O_2 to $O_2^{\cdot-}$, which could then dismutate (either spontaneously or enzymatically) to form H_2O_2 . The resulting increases in steady-state levels of $O_2^{\cdot-}$ to H_2O_2 could then diffuse through the B9 cells forming more powerful oxidants, such as hydroxyl radicals through Haber-Weiss-driven Fenton chemistry as well as organic hydroperoxides capable of causing

chronic metabolic oxidative stress and genomic instability. The B9 cells would be expected to respond to this condition of metabolic oxidative stress by increasing SOD activity (to reduce steady-state levels O_2^-) and GSH metabolism (to reduce steady-state levels of hydroperoxides via GSH peroxidases). The data obtained in this study are completely consistent with this interpretation as are previous studies with hamster fibroblasts chronically exposed to H_2O_2 (>200 $\mu\text{mol/L}$). Cells used in all of these studies showed genomic instability characterized by dramatic increases in aneuploidy (22), increased SOD activity (33), and increased GSH metabolism (34) that was clearly associated with the development of resistance to oxidative stress (11, 35, 36).

In addition, the regeneration of GSH from GSSG (formed by hydroperoxide metabolism via GSH peroxidases) requires reducing equivalents from NADPH, which is regenerated from glucose metabolism in the pentose phosphate cycle (5). In addition, pyruvate, formed at the end of glycolysis, scavenges H_2O_2 and other hydroperoxides (5). Because glucose metabolism is integrally related to hydroperoxide removal, glucose consumption would be expected to increase in B9 cells, and this was confirmed in the current study (Table 1). In addition, consistent with this interpretation, B9 cells expressing the *SDHC* mutation were found to be more sensitive to glucose deprivation-induced cytotoxicity (relative to B1; Table 1), which has been associated previously with metabolic oxidative stress (5).

To our knowledge, the current study is the first to show conclusively that a mutation in the gene coding for *SDHC* causes

increases in steady-state levels of O_2^- and aneuploidy in intact mammalian cells that can be reversed by expression of the WT *SDHC*. These results strongly support the hypothesis that mutations in genes coding for METC proteins that result in increased steady-state levels of O_2^- create a condition of chronic metabolic oxidative stress that is capable of contributing to genomic instability and other phenotypic changes associated with the cancer cells. Finally, these studies allow for the speculation that determining mutations that lead to increased steady-state levels of ROS in mammalian cells (as well as their biological consequences) may provide invaluable insights into a fundamental relationship between genetics and metabolism that contributes to the exponential increase in the incidence of degenerative diseases associated with aging (including cancer).

Acknowledgments

Received 3/3/2006; revised 5/18/2006; accepted 5/26/2006.

Grant support: NIH grants R01-CA100045, P01-CA66081, R01-CA111365, P30-CA086862, and F32-CA110611 and Department of Energy grant DE-FG02-05ER64050.

The costs of publication of this article were defrayed in part by the payment of page charges. This article must therefore be hereby marked *advertisement* in accordance with 18 U.S.C. Section 1734 solely to indicate this fact.

We thank Dr. L.W. Oberley for his helpful discussions during the project, Chris Andreopoulos and Dr. Balaraman Kalyanaram (Free Radical Research Center, Medical College of Wisconsin, Milwaukee, WI) for HPLC analysis of DHE oxidation products, Dr. Immo E. Scheffler for the B1 and B9 cell lines, Justin Fishbaugh and Gene Hess for their technical assistance with flow cytometry, Ling Li and Jeff Kirsch for technical assistance with biochemical analysis and plasmid construction, and Kellie Bodeker for her editorial assistance.

References

- Sies H. Oxidative stress: from basic research to clinical application. *Am J Med* 1991;91:31-8S.
- Hunt CR, Sim JE, Featherstone T, et al. Genomic instability and catalase gene amplification induced by chronic exposure to oxidative stress. *Cancer Res* 1998;58:3986-92.
- Finkel T, Holbrook NJ. Oxidants, oxidative stress, and the biology of ageing. *Nature* 2000;408:239-47.
- Oberley LW. In: *Superoxide dismutase*. Vol. II. Boca Raton (FL): CRC Press, Inc.; 1982. p. 127.
- Spitz DR, Sim JE, Ridnour LA, Galoforo SS, Lee YJ. Glucose deprivation-induced oxidative stress in human tumor cells. A fundamental defect in metabolism? *Ann N Y Acad Sci* 2000;899:349-62.
- Boveris A. Mitochondrial production of superoxide radical and hydrogen peroxide. *Adv Exp Med Biol* 1977;78:67-82.
- Boveris A, Cadenas E. In: Oberley LW, editors. *Superoxide dismutase*. Vol. II. Boca Raton (FL): CRC Press, Inc.; 1982. p. 15-30.
- Turrens JF, Alexandre A, Lehninger AL. Ubisemiquinone is the electron donor for superoxide formation by complex III of heart mitochondria. *Arch Biochem Biophys* 1985;237:408-14.
- Ahmad IM, Aykin-Burns N, Sim JE, et al. Mitochondrial O_2^- and H_2O_2 mediate glucose deprivation-induced cytotoxicity and oxidative stress in human cancer cells. *J Biol Chem* 2005;280:4254-63.
- Ishii T, Yasuda K, Akatsuka A, et al. A mutation in the *SDHC* gene of complex II increases oxidative stress, resulting in apoptosis and tumorigenesis. *Cancer Res* 2005;65:203-9.
- Spitz DR, Azzam EI, Li JJ, Gius D. Metabolic oxidation/reduction reactions and cellular responses to ionizing radiation: a unifying concept in stress response biology. *Cancer Metastasis Rev* 2004;23:311-22.
- Schiavi F, Boedeker CC, Baush B, et al. Predictions and prevalence of paraganglioma syndrome associated with mutations of the *SDHC* gene. *JAMA* 2005;294:2057-63.
- Baysal BE, Ferrell RE, Willett-Brozick JE, et al. Mutations in *SDHD*, a mitochondrial complex II gene, in hereditary paraganglioma. *Science* 2000;287:848-51.
- Gimm O, Armanios M, Dziema H, Neumann HP, Eng C. Somatic and occult germ-line mutations in *SDHD*, a mitochondrial complex II gene, in nonfamilial pheochromocytoma. *Cancer Res* 2000;60:6822-5.
- Gimenez-Roqueplo AP, Favier J, Rustin P, et al. Mutations in the *SDHB* gene are associated with extra-adrenal and/or malignant pheochromocytomas. *Cancer Res* 2003;63:5615-21.
- Ackrell BA. Cytopathies involving mitochondrial complex II. *Mol Aspects Med* 2002;23:369-84.
- Oostveen FG, Au HC, Meijer PJ, Scheffler IE. A Chinese hamster mutant cell line with a defect in the integral membrane protein CII-3 of complex II of the mitochondrial electron transport chain. *J Biol Chem* 1995;270:26104-8.
- Li WG, Miller FJ, Jr., Zhang HJ, Spitz DR, Oberley LW, Weintraub NL. H_2O_2 -induced O_2^- production by a non-phagocytic NAD(P)H oxidase causes oxidant injury. *J Biol Chem* 2001;276:29251-6.
- Zhao H, Joseph J, Fales HM, et al. Detection and characterization of the product of hydroethidine and intracellular superoxide by HPLC and limitations of fluorescence. *Proc Natl Acad Sci U S A* 2005;102:5727-32.
- Spitz DR, Oberley LW. An assay for superoxide dismutase activity in mammalian tissue homogenates. *Anal Biochem* 1989;179:8-18.
- Griffith OW. Determination of glutathione and glutathione disulfide using glutathione reductase and 2-vinylpyridine. *Anal Biochem* 1980;106:207-12.
- Spitz DR, Mackey MA, Li GC, Elwell JH, McCormick ML, Oberley LW. Relationship between changes in ploidy and stable cellular resistance to hydrogen peroxide. *J Cell Physiol* 1989;139:592-8.
- Sarsour EH, Agarwal M, Pandita TK, Oberley LW, Goswami PC. Manganese superoxide dismutase protects the proliferative capacity of confluent normal human fibroblasts. *J Biol Chem* 2005;280:18033-41.
- Oberley LW, Oberley TD. Role of antioxidant enzymes in cell immortalization and transformation. *Mol Cell Biol* 1988;8:4147-53.
- St. Clair DK, Oberley LW. Manganese superoxide dismutase expression in human cancer cells: a possible role of mRNA processing. *Free Radic Res Commun* 1991;12-13 Pt 2:771-8.
- Fridovich I. The biology of oxygen radicals. *Science* 1978;201:875-80.
- McCord JM, Fridovich I. The biology and pathology of oxygen radicals. *Ann Intern Med* 1978;89:122-7.
- Oberley LW, Buettner GR. Role of superoxide dismutase in cancer: a review. *Cancer Res* 1979;39:1141-9.
- Oberley LW, Oberley TD. In: Johnson JE, Jr., Walford R, Harmon D, Miquel J, editors. *Free radicals, aging, and degenerative diseases*. New York: Alan R. Liss, Inc; 1986. p. 325-81.
- Ishii N, Fujii M, Hartman PS, et al. A mutation in succinate dehydrogenase cytochrome *b* causes oxidative stress and ageing in nematodes. *Nature* 1998;394:694-7.
- Jackson AL, Loeb LA. The contribution of endogenous sources of DNA damage to the multiple mutations in cancer. *Mutat Res* 2001;477:7-21.
- Yankovskaya V, Horsefield R, Tornroth S, et al. Architecture of succinate dehydrogenase and reactive oxygen species generation. *Science* 2003;299:700-4.
- Spitz DR, Elwell JH, Sun Y, et al. Oxygen toxicity in control and H_2O_2 -resistant Chinese hamster fibroblast cell lines. *Arch Biochem Biophys* 1990;279:249-60.
- Spitz DR, Malcolm RR, Roberts RJ. Cytotoxicity and metabolism of 4-hydroxy-2-nonenal and 2-nonenal in H_2O_2 -resistant cell lines. Do aldehydic by-products of lipid peroxidation contribute to oxidative stress? *Biochem J* 1990;267:453-9.
- Spitz DR, Adams DT, Sherman CM, Roberts RJ. Mechanisms of cellular resistance to hydrogen peroxide, hyperoxia, and 4-hydroxy-2-nonenal toxicity: the significance of increased catalase activity in H_2O_2 -resistant fibroblasts. *Arch Biochem Biophys* 1992;292:221-7.
- Spitz DR, Kinter MT, Roberts RJ. Contribution of increased glutathione content to mechanisms of oxidative stress resistance in hydrogen peroxide resistant hamster fibroblasts. *J Cell Physiol* 1995;165:600-9.